Journal of Biotechnology 205 (2015) 93–100

Contents lists available at ScienceDirect

Journal of Biotechnology

journal homepage: www.elsevier.com/locate/jbiotec

# A novel *in vitro* permeability assay using three-dimensional cell culture system

Jong Bong Lee[a,1], Sung Hwa Son[b,1], Min Chul Park[b,c,1], Tae Hwan Kim[a], Min Gi Kim[a], Sun Dong Yoo[a,*], Sunghoon Kim[b,d,**]

[a] School of Pharmacy, Sungkyunkwan University, Suwon, Gyeonggi-do 440-746, Republic of Korea
[b] Medicinal Bioconvergence Research Center, Seoul National University, Seoul 151-742, Republic of Korea
[c] Advanced Institutes of Convergence Technology, Seoul National University, Suwon, Gyeonggi-do 443-270, Republic of Korea
[d] Department of Molecular Medicine and Biopharmaceutical Sciences, Graduate School of Convergence Technology, College of Pharmacy, Seoul National University, Seoul 151-742, Republic of Korea

ARTICLE INFO

*Article history:*
Received 14 August 2014
Received in revised form
10 December 2014
Accepted 19 December 2014
Available online 26 December 2014

*Keywords:*
3D cell culture
Tumor spheroids
Caco-2 cells
Drug permeability assay
Pharmacokinetics

ABSTRACT

Three-dimensional (3D) cell culture systems are well-known to better represent the *in vivo* environment and they are applied to many areas of research. Spheroid model is one of the systems of 3D cell culture and here in our research, a permeability assay utilizing the spheroids was developed. Number of cells forming the spheroids, initial compound concentration, and incubation time were optimized to provide the best assay performance. After development of the assay, it was evaluated with 22 commercially available compounds. The developed Caco-2 3D spheroid permeability assay demonstrated a reasonable correlation with human absorption values. The parallel artificial membrane permeability assay (PAMPA) was also performed for the same set of compounds and the results were compared with those of the 3D permeability assay. The correlation with human absorption values was shown to be improved with the 3D permeability assay. The successful development of the Caco-2 3D spheroid permeability assay also suggests the potential application of the 3D cell culture systems to other areas of pharmacokinetic research.



## 1. Introduction

Of many important characteristics of drug candidates, permeability is an essential parameter that needs precise and efficient assays for prediction during drug discovery. Permeability is also a critical factor contributing to the pharmacokinetic properties of compounds including absorption, distribution, metabolism and excretion (ADME). Although absorption mainly contributes to the permeability of compounds, it can manifest substantial effects on efficacy and toxicity as well. The use of *in vivo* or *in situ* animal models in permeability assessment raises unavoidable ethical concerns and presents difficulty to apply to high throughput screening. Therefore, there is increasing dependency on *in vitro* studies to evaluate drug permeability and numerous research programs have striven to develop expedient *in vitro* assays for measurement and prediction (Alsenz and Haenel, 2003; Corti et al., 2006; Gombar et al., 2003; Liu et al., 2003; Masungi et al., 2008).

Although a number of *in vitro* assays have been developed to determine the drug permeability, the results of some compounds showed low correlation with those of *in vivo* assay. For example, a permeability assay with monolayer Caco-2 cells has served as the gold standard for many years and considerable efforts have been put to improve its preciseness and convenience. Accelerated Caco-2 cell assays are available in easy-to-assay kit forms and researchers have also tried to change the cell line to a more vigorously proliferating one such as Madin–Darby canine kidney (MDCK) cells. The technology of parallel artificial membrane permeability assay (PAMPA) has also thrived and various types of membranes are used to accommodate a range of purposes. However, these assays present inherent limitations in providing promising and reliable predictions. Correlations do exist to a certain extent but still many

* Corresponding author at: School of Pharmacy, Sungkyunkwan University, 2066, Seobu-ro, Jangan-gu, Suwon-si, Gyeonggi-do 440-746, Republic of Korea. Tel.: +82 31 290 7717; fax: +82 31 290 7767.
** Corresponding author at: College of Pharmacy, Seoul National University, Gwanak-ro 1, Gwanak-gu, Seoul 151-742, Republic of Korea. Tel.: +82 2 880 8180; fax: +82 2 875 2621.
*E-mail addresses:* sdyoo@skku.ac.kr (S.D. Yoo), sungkim@snu.ac.kr (S. Kim).
[1] These authors contributed equally to this work.

http://dx.doi.org/10.1016/j.jbiotec.2014.12.019
0168-1656/

outliers bring skeptical points of view (Alsenz and Haenel, 2003; Chen et al., 2008; Liang et al., 2000; Liu et al., 2003; Masungi et al., 2008; Zhu et al., 2002).

3D cell culture has been well renowned as a technology for an *in vitro* system that mimics the *in vivo* environments better than classic two-dimensional (2D) cell culture (Abbott, 2003; Smalley et al., 2006). Among many different types of 3D cell cultures, spheroid model is simple and shows *in vivo*-mimic results in drug efficacy tests. When cells are seeded in an ultra-low attachment plate, they form a spheroid by self-assembly (Achilli et al., 2012; Youssef et al., 2011). Spheroid expresses cytokines, cell signaling molecules and drug responses in levels that resemble the *in vivo* conditions more than those of 2D cultured cells. For example, liver-specific functions, including albumin production and CYP450 activity, are induced in hepatocyte spheroids. Since spheroid also represents the natural cell structure and morphology, which are not reproducible in 2D culture systems, it exhibits *in vivo*-like physical properties (Kim, 2005). For example, cancer spheroids show gradient characteristics: from the outer layer to the inner core, there are decreases in nutrients, oxygen and cell proliferation. These properties reflect realistic cancer microenvironment. These features of the spheroids allow them to be used during drug development with regard to their characteristics of resistance, uptake, penetration, efficacy, toxicity and metabolism (Elliott and Yuan, 2011; Kim, 2005; Minchinton and Tannock, 2006; Smalley et al., 2006; Brandon et al., 2003). In this study, we sought to apply this mimicry of the spheroids on permeability studies.

There are several studies that have tried to explore the advantages of 3D cell cultures for drug characteristics. Those studies exploiting 3D cell cultures include assays with the multilayer culture and also the spheroids of cells (Haraguchi et al., 2010; Hatherell et al., 2011; Kyle et al., 2004). Some of them have tried to correlate drug penetration with the efficacy of the drug, where they were able to develop a model and examined the model with application to a single drug, doxorubicin (Shin et al., 2013). Here in our research, we developed a novel *in vitro* permeability assay utilizing the 3D spheroids of Caco-2 cells and applied to commercially available compounds to evaluate the appropriateness of the assay for permeability prediction. PAMPA was also performed on the same set of compounds and the results were compared.

## 2. Materials and methods

### 2.1. Cell culture and materials

Human colon cancer cell line, Caco-2, obtained from American Type Culture Collection (ATCC), were cultured in Dulbecco's modified Eagle's medium (DMEM, Hyclone) supplemented with 10% fetal bovine serum (FBS, Hyclone) and 1% penicillin/streptomycin and maintained in a humidified 5% $CO_2$ incubator at 37 °C. All compounds were purchased from Sigma–Aldrich. HPLC grade acetonitrile and water were purchased from J.T. Baker and Dulbecco's phosphate buffered saline (DPBS) from Hyclone.

### 2.2. 3D cell culture

For 3D cell culture, 2D cultured cells were dissociated as a single cell by cell detachment buffer, Accumax (Millipore), and then the cell number was calculated by C-Chip hemacytometer (INCYTO). Suspended-cells were seeded in ultra-low attachment 96-well plates (Lipidure-Coat Plate, NOF Corp., Japan). After 3 days, the cultured media were replaced with the growth medium containing compounds for the assays. Each compound was dissolved in dimethyl sulfoxide (DMSO) as a 25 mM stock and 4 μl of the stock was added to 496 μl of medium to yield 200 μM of compound in the medium. This medium containing 200 μM of compound was serially diluted to produce desired concentrations for each specific experiment. Half volume of culture media (50 μl) was replaced with compound containing medium on day 3. In replacement step, the compound was diluted to 1:2 for final concentration. After pre-determined incubation times, 50 μl of medium and spheroids were harvested from each well for LC–MS/MS analysis. Each collected spheroid was dropped into a well containing 200 μl of DPBS for washing purposes. Washing with DPBS was repeated three times by 500 g centrifugation to remove the culture medium to ensure accurate concentration analysis. Then the spheroid was put into 200 μl of acetonitrile containing internal standard for sample preparation and analysis. For 3D spheroid imaging, the images of spheroids were observed by phase contrast imaging on a Nikon Eclipse Ti inverted microscope. The spheroid area was measured using a Nikon microscopy program.

### 2.3. Cell viability assay

Cell viability analysis was performed with cells cultured on 2D and 3D culture 96 well plates by CellTiter-Glo Luminescent Cell Viability Assay (Promega). After desired incubation conditions, 100 μl of CellTiter-Glo solution was added to each well and the plate was incubated at room temperature for 30 min with gentle shaking. Each well was analyzed with a FLUOstar OPTIMA multi-mode microplate reader (BMG Labtech) and numbers of viable cells were determined according to manufacturer's instructions. All experiments were performed in triplicate.

### 2.4. Immunofluorescence analysis

Immunofluorescence analysis was performed with spheroids after 3 days incubation. Each spheroid was embedded in optimal cutting temperature compound (Tissue-Tek OCT, Sakura), and frozen immediately by liquid nitrogen. The frozen samples were serially sectioned with thickness of 10 μm by microtome (Thermal Scientific) and stained with 4′,6-diamidino-2-phenylindole (DAPI). Images were obtained using confocal microscopy (Nikon, A1).

### 2.5. Quantitative real-time PCR

RNA of spheroid was extracted using RNeasy Mini Kit (Qiagen) and the RNA was reverse transcribed into cDNA using Maxima First Strand (Thermo-scientific). For real-time PCR amplification, 500 ng of cDNA was used as a template. PCR amplification was performed on a 7500 Real time PCR system (Applied Biosystems) with maxima-SYBR (Thermo-scientific). The PCR conditions were as follows: 40 cycles of 15 s at 95 °C followed by 1 min at 58 °C. The primer sequences are shown in Supplementary Table S1. Relative expression levels of target genes were calculated by the $\Delta\Delta C_T$ method with GAPDH used as a reference gene.

Supplementary Table S1 related to this article can be found, in the online version, at http://dx.doi.org/10.1016/j.jbiotec.2014.12.019.

### 2.6. LC–MS/MS analysis

Drug concentrations were determined by LC–MS/MS using an API 2000 triple quadrupole mass spectrometer with an electrospray ionization (ESI) source (AB MDS Sciex) coupled to Alliance 2690 HPLC system (Waters). The basic parameters for the coupled system were applied as previously described elsewhere with minor modifications per each compound (Kim et al., 2012; Shin et al., 2009). When the ESI source was operated in positive mode, the mobile phase was constituted of acetonitrile with 0.1% formic acid and distilled water, 70:30 (v/v), with nonivamide as the internal standard.

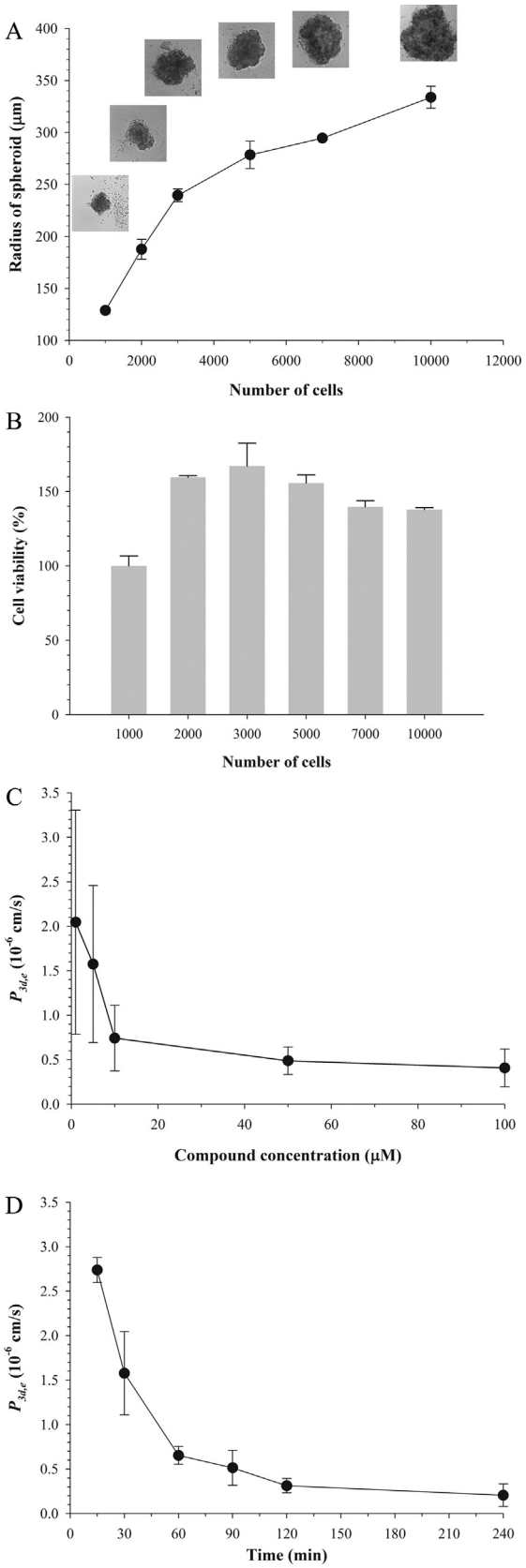


**Fig. 1.** Optimization results of the Caco-2 3D spheroid permeability assay. (A) Mean sizes for spheroids with different numbers of cells forming the spheroids are plotted with respective image examples of the spheroids. (B) Viabilities of cells are plotted against number of cells. Viability from 1000 cells/well has been set as 100%. (C) $P_{3d,e}$ values are plotted against initial concentration of test compounds. (D) $P_{3d,e}$ values are plotted against incubation time of the spheroids.

In the other hand, when the ESI source was operated in negative mode, 10 mM ammonium acetate and distilled water, 60:40 (v/v), was used as mobile phase and flurbiprofen as the internal standard. Flow rate was 0.3 ml/min for both modes of ESI source. For determination of drug concentration in the spheroid, it was put into 200 μl of acetonitrile containing 200 ng/ml of nonivamide or flurbiprofen and the mixture was vortexed for 30 s for disintegration and deproteinization of the spheroids. Then, the mixture was filtered with the AcroPrep 96 filter plates (Pall) before injection of 20 μl into the HPLC system. Preparation of samples from medium was similar except that 20 μl of medium was used for each sample. Calibration curves were constructed at a range of 50 nM–50 μM and 500 nM–50 μM for the compounds with higher and lower signal intensity, respectively. The lower limit of quantification was determined at the concentration which yielded a signal-to-noise ratio of >10. All calibration curves were required to meet $r^2 > 0.999$ and accuracy ≤15% to be eligible for quantification.

### 2.7. Calculation of efficient permeability

To calculate the efficient permeability ($P_{3d,e}$) of Caco-2 3D spheroid permeability assay, a modified $P_e$ equation of PAMPA was used as below:

$$P_{3d,e} = \frac{-\ln(1 - C_S/C_{equilibrium}}{A_S \times (1/V_M + 1/V_S) \times t}$$

where $C_S$ is the compound concentration in the spheroid (acceptor) at time $t$, $A_S$ is the surface area of the spheroid, $V_M$ is the volume of medium (donor), $V_S$ is the volume of spheroid, and $t$ is the incubation time. $C_{equilibrium}$ is obtained by the following equation:

$$C_{equilibrium} = \frac{C_M \cdot V_M + C_S \cdot V_S}{V_M + V_S}$$

where $C_M$ is the compound concentration in the medium at time $t$.

### 2.8. Parallel artificial membrane permeability assay (PAMPA)

PAMPA was conducted with a pre-coated PAMPA 96-well plate system (BD Gentest, Cat no. 353015) following the manufacturer's instructions. Briefly, 300 μl of DPBS (pH 7.4) was added to each well of the receiver plate, and 200 μl of DPBS (pH 7.4) containing 50 μM of the test compound was added to each well of the filter plate. After the system was incubated at room temperature for 4 h without shaking, the samples from both plates were obtained for analysis. A humidity maintained incubator was not needed because the evaporation was negligible with a short incubation time. Efficient permeability ($P_e$) was calculated with the following equation:

$$P_e = \frac{-\ln(1 - C_A/C_{equilibrium})}{A \times (1/V_D + 1/V_A) \times t}$$

where $C_A$ is the compound concentration in the receiver well (acceptor) at time $t$, $A$ is the surface area of the filter, $V_D$ is the volume of filter well (donor), $V_A$ is the volume of receiver well, and $t$ is the incubation time. $C_{equilibrium}$ is in this case obtained by the following equation:

$$C_{equilibrium} = \frac{C_D \cdot V_D + C_A \cdot V_A}{V_D + V_A}$$

where $C_D$ is the compound concentration in the filter well at time $t$.

**Table 1**
Sizes of spheroids from assay by compound concentration (μm, $n = 3$ each).

| Conc. (μM) | Desipramine | Nadolol | Ranitidine | Terbutaline | Total |
|---|---|---|---|---|---|
| 0 | 264.0 ± 1.3 | 269.4 ± 12.9 | 249.4 ± 7.1 | 268.8 ± 7.3 | 262.9 ± 11.0 |
| 1 | 265.7 ± 8.7 | 264.3 ± 3.9 | 250.6 ± 7.9 | 250.6 ± 7.9 | 261.9 ± 9.5 |
| 5 | 257.0 ± 7.4 | 262.4 ± 7.2 | 257.3 ± 3.7 | 257.3 ± 3.7 | 261.2 ± 7.4 |
| 10 | 261.7 ± 9.3 | 262.2 ± 4.4 | 260.8 ± 5.7 | 260.8 ± 5.7 | 263.6 ± 8.1 |
| 50 | 264.3 ± 3.9 | 269.9 ± 5.9 | 272.0 ± 7.0 | 272.0 ± 7.0 | 267.7 ± 7.1 |
| 100 | 258.6 ± 0.4 | 274.1 ± 7.9 | 263.7 ± 4.5 | 263.7 ± 4.5 | 267.8 ± 7.6 |
| Mean ± SD of all samples | | 264.1 ± 8.7 | Coefficient of variation (%) | | 3.3 |

**Table 2**
List of compounds tested.

| *Compounds* | MW | $F_a$ in human (%)[a] | $P_{3d,e}$ ($10^{-6}$ cm/s)[b] | PAMPA $P_e$ ($10^{-6}$ cm/s)[b] | ESI source mode | Cell viability (%)[b] | |
|---|---|---|---|---|---|---|---|
| | | | | | | 2D culture | 3D culture |
| Acebutolol | 336.4 | 90 | 0.28 ± 0.05 | 3.62 ± 1.07 | + | 103.0 ± 4.4 | 108.0 ± 1.9 |
| Acyclovir | 225.2 | 21 | 0.14 ± 0.04 | 4.63 ± 1.63 | + | 99.9 ± 3.1 | 94.6 ± 3.5 |
| Alprenolol | 249.3 | 94 | 0.36 ± 0.04 | 31.95 ± 2.17 | + | 100.5 ± 2.9 | 103.7 ± 3.4 |
| Atenolol | 266.3 | 52 | 0.12 ± 0.02 | 11.50 ± 6.44 | + | 99.2 ± 3.4 | 113.9 ± 17.0 |
| Bretylium | 243.2 | 22 | 0.13 ± 0.07 | 0.87 ± 0.80 | + | 96.3 ± 3.6 | 98.5 ± 2.7 |
| Cimetidine | 252.3 | 93 | 0.21 ± 0.10 | 4.74 ± 1.85 | + | 99.1 ± 3.1 | 96.9 ± 1.6 |
| Clonidine | 230.1 | 96 | 0.21 ± 0.03 | 23.27 ± 2.72 | + | 99.7 ± 2.2 | 100.7 ± 11.6 |
| Desipramine | 266.4 | 100 | 1.17 ± 0.52 | 27.49 ± 6.55 | + | 99.8 ± 4.3 | 114.4 ± 22.1 |
| Diclofenac | 296.1 | 100 | 0.48 ± 0.14 | 25.30 ± 1.52 | – | 101.0 ± 1.7 | 101.3 ± 2.7 |
| Diltiazem | 414.5 | 92 | 0.32 ± 0.04 | 38.73 ± 2.35 | + | 98.0 ± 4.1 | 99.5 ± 4.4 |
| Enalapril | 376.4 | 60 | 0.15 ± 0.03 | 6.56 ± 0.79 | – | 97.1 ± 1.0 | 100.8 ± 4.4 |
| Furosemide | 330.8 | 60 | 0.10 ± 0.07 | 5.66 ± 2.07 | – | 95.9 ± 3.1 | 115.3 ± 16.9 |
| Imipramine | 280.4 | 99 | 0.49 ± 0.17 | 31.46 ± 5.30 | + | 95.7 ± 1.4 | 101.9 ± 4.8 |
| Indomethacin | 357.8 | 100 | 0.24 ± 0.02 | 15.93 ± 2.26 | – | 98.7 ± 3.2 | 107.4 ± 13.9 |
| Nadolol | 309.4 | 32 | 0.03 ± 0.00 | 11.26 ± 3.36 | + | 94.8 ± 4.3 | 105.9 ± 4.9 |
| Naproxen | 230.3 | 98 | 0.25 ± 0.10 | 14.01 ± 2.43 | – | 97.0 ± 3.2 | 110.5 ± 8.5 |
| Piroxicam | 331.4 | 100 | 0.05 ± 0.02 | 15.29 ± 2.41 | + | 98.5 ± 4.3 | 105.0 ± 3.1 |
| Ranitidine | 314.4 | 55 | 0.03 ± 0.00 | 5.12 ± 1.94 | + | 93.2 ± 2.5 | 100.4 ± 2.6 |
| Salicylic acid | 138.1 | 100 | 0.33 ± 0.15 | 6.81 ± 0.39 | – | 95.6 ± 2.7 | 106.3 ± 11.0 |
| Sulfasalazine | 398.4 | 12 | 0.13 ± 0.03 | 4.87 ± 0.99 | + | 98.0 ± 2.5 | 108.9 ± 8.0 |
| Terbutaline | 225.3 | 68 | 0.13 ± 0.02 | 7.43 ± 2.73 | + | 99.4 ± 3.8 | 105.1 ± 0.8 |
| Verapamil | 454.6 | 98 | 0.80 ± 0.44 | 29.16 ± 3.13 | + | 98.8 ± 4.7 | 101.9 ± 1.8 |

[a] Referenced from Zhu et al. (2002).
[b] Data shown as mean ± SD from at least $n = 3$.

## 3. Results and discussion

### 3.1. Optimization of spheroid size

To form spheroids for the permeability test, Caco-2 cells were seeded in the ultra-low attachment 96-well plates with a round bottom coated with 2-methacryloyloxy-ethyl-phosphorylcholine (Eiraku et al., 2011). Cells spontaneously formed a single spheroid by self-assembly and gravity force in each well. Since spheroids incubated for 3 days were stable and healthy, they were used for the permeability assay. Factors affecting drug permeability were optimized to set up the experimental conditions. First, a range of cell numbers was tested to find the reliable and *in vivo*-mimic conditions for the permeability assay. Six different numbers of cells, from 1000 to 10,000 cells per well, were seeded to the 3D culture plates. After 3 days of incubation in the 3D culture plates, the images of spheroids were observed to determine the spheroid size (Fig. 1A). Spheroid sizes and cell numbers showed a positive correlation. Since the critical passive diffusion distance is 100 μm (Hirschhaeuser et al., 2010), spheroid size of larger than 200 μm was used to determine the permeability. As seen with the images, the spheroid sizes formed with low cell numbers (1000–3000 cells/well) were smaller than 200 μm and were inadequate for permeability assay. The spheroids formed with high cell numbers (7000–10,000 cells/well) did not form evenly shaped spheroids and the clusters of cells were frequently observed. The medium cell number (5000 cells/well) provided adequate spheroid size and was used in subsequent studies. To determine viability of cells, spheroids were formed with six different numbers of cells from 1000 to 10,000 cells per well and the numbers of viable cells were determined after 3 days of incubation. The number of viable cells increased with the number of cells seeded but reached a saturated level (Fig. 1B). These results also support that 5000 cells/well is a reasonable number of cells to be used for spheroid formation.

### 3.2. Compound concentration for permeability assay

For the optimization of compound concentration for the assay, four different drugs of desipramine, nadolol, terbutaline and ranitidine were tested over a wide range of concentrations (1–100 μM). Since these compounds showed a wide spectrum of human $F_a$ (range, 32–100%) and did not fall into a single scaffold group, they were selected as the test compounds. After 3 days of incubation, spheroids were treated with these compounds for 2 h. To determine the compound concentration, spheroids and cultured media were harvested for LC–MS/MS analysis. Drug concentration analysis was performed on the spheroids and media to obtain $P_{3d,e}$. The $P_{3d,e}$ was calculated by the modified PAMPA $P_e$ equation. The $P_{3d,e}$ of these compounds have been adjusted by their own overall $P_{3d,e}$ to avoid bias of compounds with higher absolute $P_{3d,e}$ having more influence on the profiles than compounds with lower absolute $P_{3d,e}$. The $P_{3d,e}$ was determined to be relatively high when the initial concentration was low

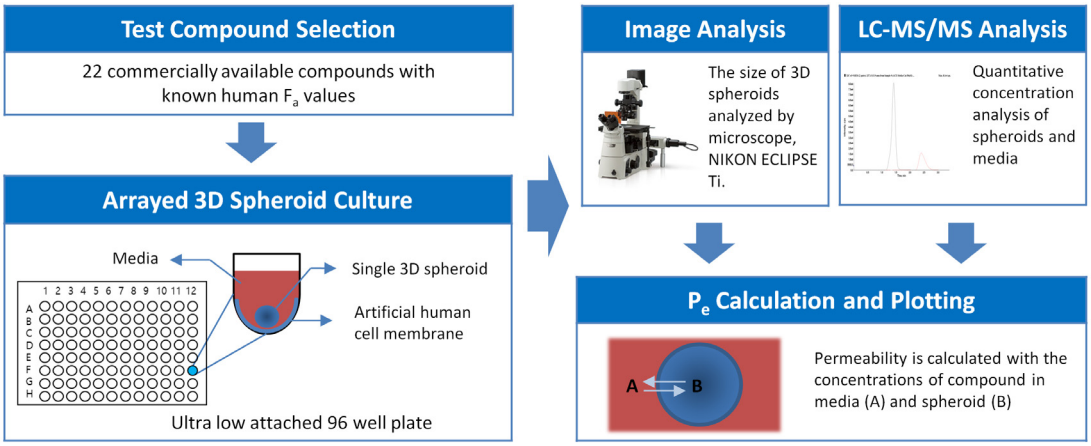


**Fig. 2.** Schematic diagram of the experimental flow.

and was decreased as the initial concentration was increasing. From these results, an initial concentration of 10 μM was used as it was the point where $P_{3d,e}$ began to show equilibrium (Fig. 1C).

Differences in compound and concentration did not appear to affect the size of the spheroids (Table 1). From the collected size data of spheroids, it could be also understood that size variation of the spheroids was negligible (coefficient of variation = 3.3%). Therefore after seeding 5000 cells/well, a spheroid with a mean radius of 264.1 μm was expected and this radius was used for the calculation of $P_{3d,e}$ of 22 commercially available drugs.

### 3.3. Incubation time for permeability assay

In order to find the relationship between $P_{3d,e}$ values and the incubation time, different time points were tested with the four different compounds as used above. Spheroids were treated at a concentration of 10 μM over a range of from 15 to 240 min. At predetermined incubation times, both spheroids and media were harvested for drug concentration analysis. The $P_{3d,e}$ was relatively high with unstable pattern during the early time of incubation. $P_{3d,e}$ values reached an equilibrium at approximately 2 h (Fig. 1D). Therefore, 2 h was selected as the optimal incubation time. Since 2 h is widely used as the incubation time, these results also promoted comparability and compatibility with other permeability assays using Caco-2 cells (Carrara et al., 2007).

### 3.4. Properties of Caco-2 3D spheroids

The relevance of properties of Caco-2 3D spheroid model to *in vivo* conditions was investigated. Morphological characteristics and biological function of the spheroids were examined. Previous literatures, using Caco-2 3D culture models, have reported hollow spheres, which mimics *in vivo* intestinal villi, with a single layer of cells along the boundary (Huh et al., 2013; Kim et al., 2014; Jagan et al., 2013). The immunofluorescence analysis result also exhibits that Caco-2 cells have aligned in a single layer along the edge of spheroid and formed a hollow multicellular spheroid structure (Supplementary Fig. S1).

Supplementary Fig. S1 related to this article can be found, in the online version, at http://dx.doi.org/10.1016/j.jbiotec.2014.12.019.

Additionally, metabolic activities of Caco-2 3D spheroids were examined. Although CYP450 enzymes play critical roles for metabolic activities of cells (Maurel, 1996), Caco-2 cell is known to display inappreciable levels of CYP expression (Prueksaritanont et al., 1996; Sambuy et al., 2005). The HepG2 cells are the most frequently used cell line to study human drug metabolic activity (Martin et al., 2010). Hewitt et al. and Maruyama et al. reported that HepG2 cells have phase 1 enzymes including CYP1A, CYP2C, and CYP3A, but their activities and levels vary depending on cell culture conditions (Hewitt and Hewitt, 2004; Maruyama et al., 2007). CYP expression levels were evaluated in 2D and 3D culture conditions of Caco-2 cells by quantitative RT-PCR. HepG2 was used as positive control. We found out that while the expression levels in HepG2 cells were detected with the performed assays, overall CYP expression levels in Caco-2 cells in both 2D and 3D culture conditions were relatively limited (Supplementary Fig. S2). Therefore, our results indicated that Caco-2 3D spheroids provide relevance to *in vivo* conditions without any outstanding issue regarding cell viabilities and metabolic activities.

Supplementary Fig. S2 related to this article can be found, in the online version, at http://dx.doi.org/10.1016/j.jbiotec.2014.12.019.

### 3.5. Correlation with human absorption values

A set of 22 commercially available FDA-approved drugs (listed in Table 2), showing structural diversity was selected for permeability assay (Fig. 2). Quantitative drug concentration analysis was performed with LC–MS/MS and examples of representative chromatograms and calibration curves used for concentration determination are shown in Fig. 3. To compare $P_{3d,e}$ with drug absorption values, previously reported human fraction absorbed ($F_a$) values of these compounds were used (Zhu et al., 2002). The assay was conducted with the optimized conditions as described above and the obtained $P_{3d,e}$ are listed in Table 2 along with the human $F_a$ values. Correlation plots of the human $F_a$ with the $P_{3d,e}$ values obtained from the Caco-2 3D spheroid permeability assay are shown in Fig. 4A. As with other permeability assays, high/low permeability ranking discriminators were used (Avdeef et al., 2007; Chen et al., 2008). A discriminator of $0.17 \times 10^{-6}$ cm/s provided a reasonable correlation for most compounds. If $P_{3d,e}$ of a tested compound is higher than $0.17 \times 10^{-6}$ cm/s, it would have a high potential of showing good absorption characteristics. Piroxicam was the only false negative outlier among the 22 compounds. Although piroxicam is readily absorbed when orally administrated, it has a small volume of distribution (Verbeeck et al., 1986). It has an apparent volume of distribution ($V_d$) of 0.12–0.14 l/kg which is commonly observed with the compounds of poor penetration through cell membranes (Ishizaki et al., 1979). These compounds exhibit $V_d$ which approximates the volume of extracellular fluid in humans (about 12 l/70 kg) indicating that they are mostly distributed in extracellular than intracellular fluid compartments

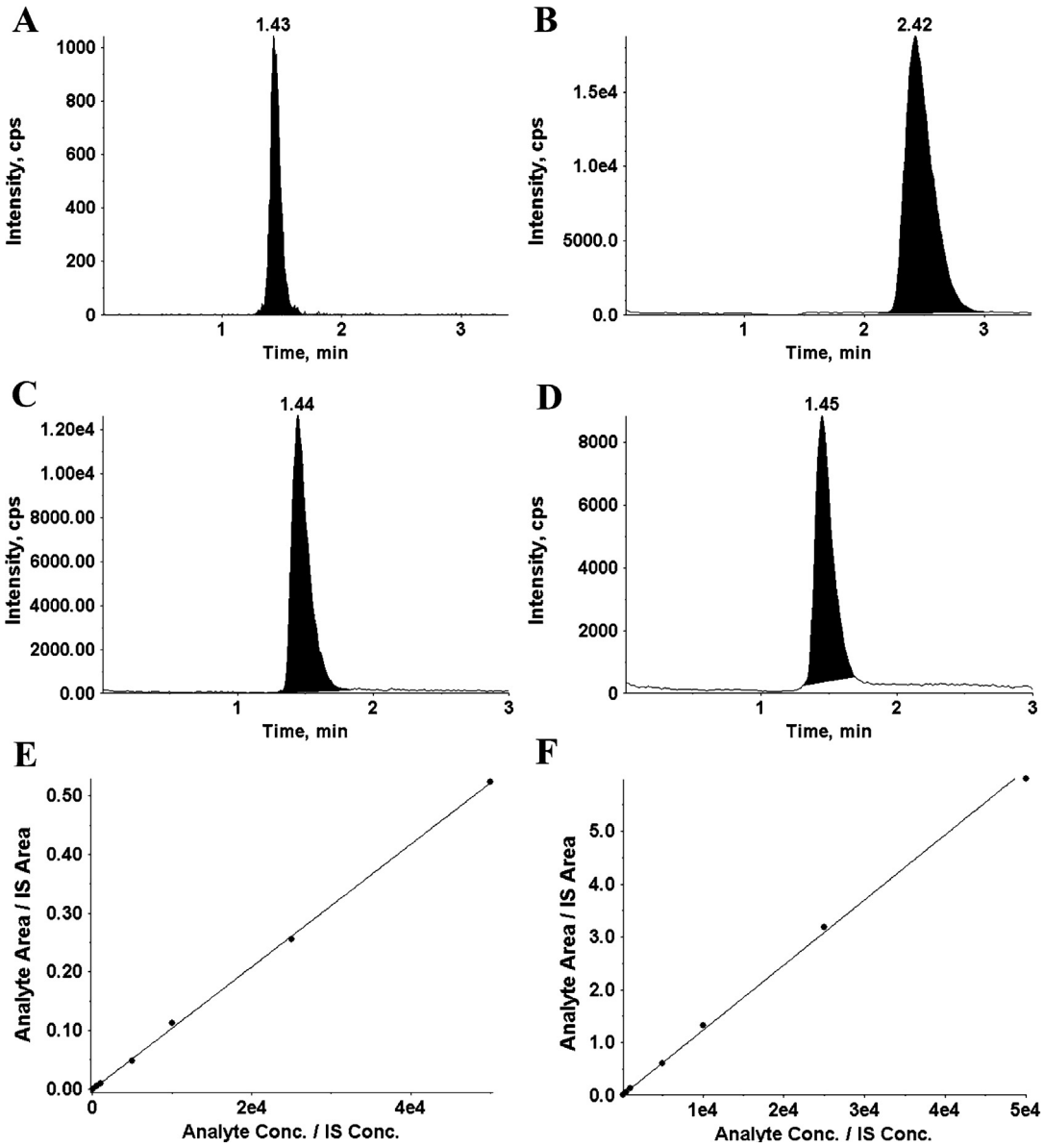


**Fig. 3.** Examples of multiple reaction monitoring chromatograms and calibration curves used for quantitative drug concentration analysis with LC–MS/MS system. (A) Chromatogram of bretylium (50 nM) used for calibration curve construction. (B) Chromatogram of nonivamide (200 ng/ml), internal standard used during ESI positive mode. (C) Chromatogram of a spheroid sample treated with naproxen (10 μM). (D) Chromatogram of flurbiprofen (200 ng/ml), internal standard used during ESI negative mode. (E) Calibration curve used for quantification of furosemide ($r^2$ = 0.9992). (F) Calibration curve used for quantification of piroxicam ($r^2$ = 0.9993).

(Vesell, 1974). Overall, the developed Caco-2 3D spheroid permeability assay provided a reasonable prediction of absorption characteristics of tested drugs.

### 3.6. Cytotoxicity of compounds

Cell viability was also determined in optimized conditions of drug permeability test to evaluate cytotoxicity. This was to assess and compare the toxicity of test compounds manifested in 2D and 3D cell culture conditions. The cells were treated with 10 μM of each compound. After 2 h incubation, the cell viability was determined. Remarkable cytotoxicity of tested drugs was not observed in 3D optimized condition (Table 2). This result demonstrated that $P_{3d,e}$ values reflect only the permeability of drugs.

### 3.7. Parallel artificial membrane permeability assay (PAMPA) and Caco-2 monolayer permeability assay

The same set of compounds tested for Caco-2 3D spheroid permeability assay was used for PAMPA. The $P_e$ values obtained from PAMPA are also listed in Table 2. From the correlation plots of human $F_a$ with $P_e$ from PAMPA, although the plots seemed reasonable, three false negative outliers were found; acebutolol, cimetidine, and salicylic acid (Fig. 4B). Additionally, correlation plots of human $F_a$ with efficient permeability values ($P_{2d,e}$) obtained from Caco-2 monolayer permeability assay reported in literature (Zhu et al., 2002) also resulted in two false negative outliers; acebutolol, cimetidine (Fig. 4C). Therefore, enhanced correlation was demonstrated with the Caco-2 3D spheroid permeability assay in this set of compounds.

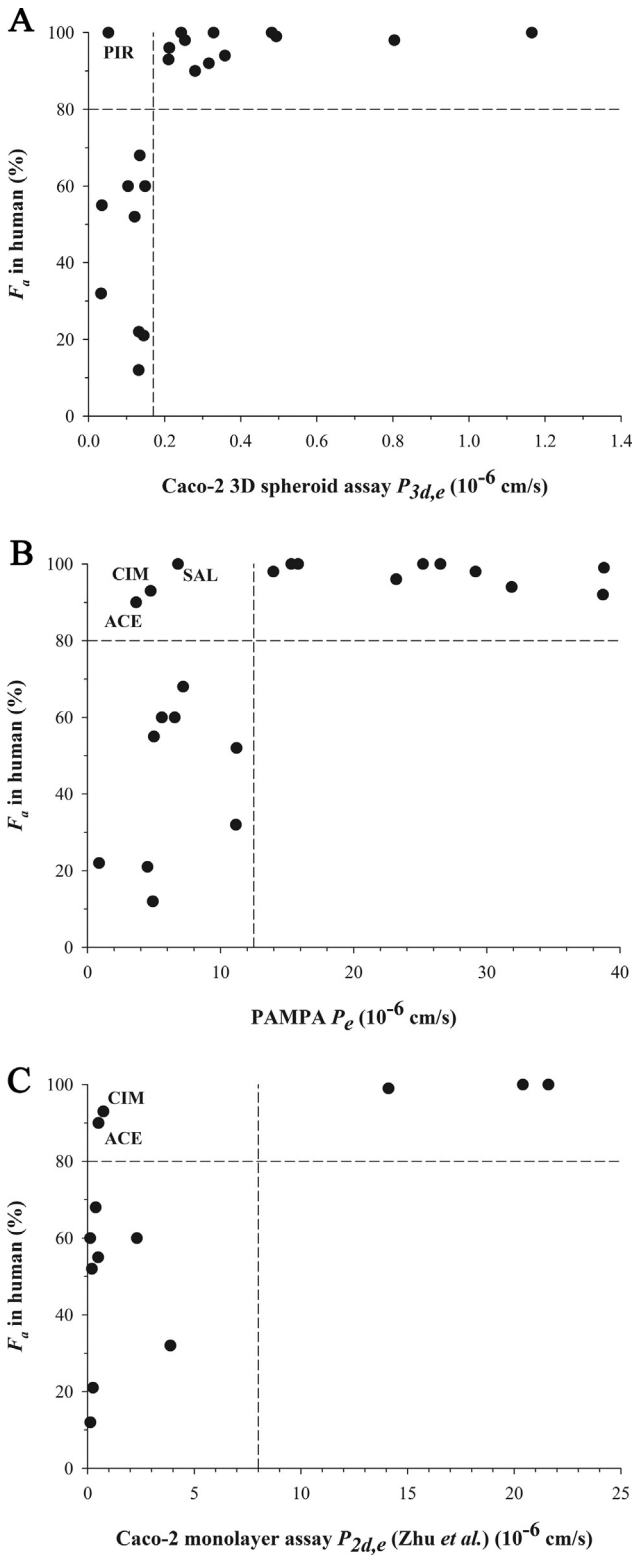


**Fig. 4.** Correlation plots of human absorption values and $P_e$ values. (A) Human $F_a$ values are plotted in correlation with $P_{3d,e}$ values from Caco-2 3D spheroid permeability assay. (B) Human $F_a$ values are plotted in correlation with $P_e$ values from PAMPA. (C) Human $F_a$ values are plotted in correlation with $P_{2d,e}$ values from Caco-2 monolayer permeability assay. $P_{2d,e}$ values are adopted from literature (Zhu et al., 2002). Vertical dotted lines represent the high/low permeability ranking discriminator for each graph. Horizontal dotted line is plotted at $F_a$ = 80% for each graph. ACE, acebutolol; CIM, cimetidine; PIR, piroxicam; SAL, salicylic acid.

## 4. Conclusion

This study describes the development and application of a novel *in vitro* permeability assay utilizing a 3D cell culture system of Caco-2 cells. An improved correlation was observed with the Caco-2 3D spheroid permeability assay compared with the existing PAMPA system. This 3D culture system is remarkable in that LC–MS/MS may be applied, which enables the quantitative analysis of the concentration permeated into the 3D spheroids compared to previous studies where visualization techniques were used. Therefore, this study demonstrates that the developed Caco-2 3D spheroid permeability assay is an efficient technique for prediction of absorption characteristics of compounds.

Given that 3D spheroid culture environment better mimics *in vivo* situation (Smalley et al., 2006) and that the spheroids manifest similar characteristics as 3D cultured intestinal epithelial villi (Huh et al., 2013; Kim et al., 2014; Jagan et al., 2013), this Caco-2 3D spheroid permeability assay may also be applied to other areas of pharmacokinetics. With enhanced prediction of absorption characteristics, it can contribute in bridging the gap between *in vitro* and *in vivo* efficacy assays. Additionally, drug interaction studies regarding efflux pumps or transporters may be performed when the media closer to the *in vivo* environments are used. Therefore this research provides an opportunity to expand the 3D cell culture systems to the area of pharmacokinetics beyond the absorption test of compounds, and also solutions in translating *in vitro* efficacy to *in vivo*.

## Author contributions

M.C.P., S.D.Y., and S.K. designed experiments. J.B.L., S.H.S., T.H.K., and M.C.P. performed experiments. J.B.L., S.H.S., M.G.K., and S.D.Y. analyzed the data. J.B.L, S.H.S., and M.C.P. wrote the manuscript. S.D.Y. and S.K. reviewed the manuscript. J.B.L., S.H.S., M.C.P., T.H.K., M.G.K., S.D.Y., and S.K. discussed the results and commented. All authors have approved the final article.

## Conflict of interest

The authors declare no competing financial interests.

## Acknowledgements

This work was supported by the Global Frontier Project (grants NRF-M3A6A4-2010-0029785) of National Research Foundation funded by the Ministry of Science, ICT & Future Planning (MSIP) of Korea. This work was also supported by a grant from Gyeonggi Research Development Program.

## References

Abbott, A., 2003. Biology's new dimension. Nature 424, 870–872.
Achilli, T.M., McCalla, S., Tripathi, A., Morgan, J.R., 2012. Quantification of the kinetics and extent of self-sorting in three dimensional spheroids. Tissue Eng. C. Methods 18, 302–309.
Alsenz, J., Haenel, E., 2003. Development of a 7-day, 96-well Caco-2 permeability assay with high-throughput direct UV compound analysis. Pharm. Res. 20, 1961–1969.
Avdeef, A., Bendels, S., Di, L., Faller, B., Kansy, M., Sugano, K., Yamauchi, Y., 2007. PAMPA – critical factors for better predictions of absorption. J. Pharm. Sci. 96, 2893–2909.
Brandon, E.F.A., Raap, C.D., Meijerman, I., Beijnen, J.H., Schellens, J.H.M., 2003. An update on in vitro test methods in human hepatic drug biotransformation research: pros and cons. Toxicol. Appl. Pharmacol. 189, 233–246.
Carrara, S., Reali, V., Misiano, P., Dondio, G., Bigogno, C., 2007. Evaluation of in vitro brain penetration: optimized PAMPA and MDCKII-MDR1 assay comparison. Int. J. Pharm. 345, 125–133.
Chen, X., Murawski, A., Patel, K., Crespi, C.L., Balimane, P.V., 2008. A novel design of artificial membrane for improving the PAMPA model. Pharm. Res. 25, 1511–1520.

Corti, G., Maestrelli, F., Cirri, M., Zerrouk, N., Mura, P., 2006. Development and evaluation of an in vitro method for prediction of human drug absorption II. Demonstration of the method suitability. Eur. J. Pharm. Sci. 27, 354–362.

Eiraku, M., Takata, N., Ishibashi, H., Kawada, M., Sakakura, E., Okuda, S., Sekiguchi, K., Adachi, T., Sasai, Y., 2011. Self-organizing optic-cup morphogenesis in three-dimensional culture. Nature 472, 51–56.

Elliott, N.T., Yuan, F., 2011. A review of three-dimensional in vitro tissue models for drug discovery and transport studies. J. Pharm. Sci. 100, 59–74.

Gombar, V.K., Silver, I.S., Zhao, Z., 2003. Role of ADME characteristics in drug discovery and their in silico evaluation: in silico screening of chemicals for their metabolic stability. Curr. Top. Med. Chem. 3, 1205–1225.

Haraguchi, Y., Sekine, W., Shimizu, T., Yamato, M., Miyoshi, S., Umezawa, A., Okano, T., 2010. Development of a new assay system for evaluating the permeability of various substances through three-dimensional tissue. Tissue Eng. C: Methods 16, 685–692.

Hatherell, K., Couraud, P.O., Romero, I.A., Weksler, B., Pilkington, G.J., 2011. Development of a three-dimensional, all-human in vitro model of the blood-brain barrier using mono-, co-, and tri-cultivation Transwell models. J. Neurosci. Methods 199, 223–229.

Hewitt, N.J., Hewitt, P., 2004. Phase I and II enzyme characterization of two sources of HepG2 cell lines. Xenobiotica 34, 243–256.

Hirschhaeuser, F., Menne, H., Dittfeld, C., West, J., Mueller-Klieser, W., Kunz-Schughart, L.A., 2010. Multicellular tumor spheroids: an underestimated tool is catching up again. J. Biotechnol. 148, 3–15.

Huh, D., Kim, H.J., Fraser, J.P., Shea, D.E., Khan, M., Bahinski, A., Hamilton, G.A., Ingber, D.E., 2013. Microfabrication of human organs-on-chips. Nat. Protoc. 8, 2135–2157.

Ishizaki, T., Nomura, T., Abe, T., 1979. Pharmacokinetics of piroxicam, a new nonsteroidal anti-inflammatory agent, under fasting and postprandial states in man. J. Pharmacokinet. Biopharm. 7, 369–381.

Jagan, I., Fatehullah, A., Deevi, R.K., Bingham, V., Campbell, F.C., 2013. Rescue of glandular dysmorphogenesis in PTEN-deficient colorectal cancer epithelium by PPARγ-targeted therapy. Oncogene 7 (32), 1305–1315.

Kim, J.B., 2005. Three-dimensional tissue culture models in cancer biology. Semin. Cancer Biol. 15, 365–377.

Kim, M.G., Shin, B.S., Choi, Y., Ryu, J.K., Shin, S.W., Choo, H.W., Yoo, S.D., 2012. Determination and pharmacokinetics of [6]-gingerol in mouse plasma by liquid chromatography-tandem mass spectrometry. Biomed. Chromatogr. 26, 660–665.

Kim, S.H., Chi, M., Yi, B., Kim, S.H., Oh, S., Kim, Y., Park, S., Sung, J.H., 2014. Three-dimensional intestinal villi epithelium enhances protection of human intestinal cells from bacterial infection by inducing mucin expression. Integr. Biol. (Camb.) 18 (6), 1122–1131.

Kyle, A.H., Huxham, L.A., Chiam, A.S., Sim, D.H., Minchinton, A.I., 2004. Direct assessment of drug penetration into tissue using a novel application of three-dimensional cell culture. Cancer Res. 64, 6304–6309.

Liang, E., Chessic, K., Yazdanian, M., 2000. Evaluation of an accelerated Caco-2 cell permeability model. J. Pharm. Sci. 89, 336–345.

Liu, H., Sabus, C., Carter, G.T., Du, C., Avdeef, A., Tischler, M., 2003. In vitro permeability of poorly aqueous soluble compounds using different solubilizers in the PAMPA assay with liquid chromatography/mass spectrometry detection. Pharm. Res. 20, 1820–1826.

Martin, P., Riley, R., Thompson, P., Williams, D., Back, D., Owen, A., 2010. Effect of prototypical inducers on ligand activated nuclear receptor regulated drug disposition genes in rodent hepatic and intestinal cells. Acta Pharmacol. Sin. 31, 51–65.

Maruyama, M., Matsunaga, T., Harada, E., Ohmori, S., 2007. Comparison of basal gene expression and induction of CYP3As in HepG2 and human fetal liver cells. Biol. Pharm. Bull. 30, 2091–2097.

Masungi, C., Mensch, J., Van Dijck, A., Borremans, C., Willems, B., Mackie, C., Noppe, M., Brewster, M.E., 2008. Parallel artificial membrane permeability assay (PAMPA) combined with a 10-day multiscreen Caco-2 cell culture as a tool for assessing new drug candidates. Pharmazie 63, 194–199.

Maurel, P., 1996. The CYP3A family. In: Ioannides, C. (Ed.), Cytochromes P450: Metabolic and Toxicological Aspects. CRC Press, Inc., Boca Raton, pp. 241–270.

Minchinton, A.I., Tannock, I.F., 2006. Drug penetration in solid tumours. Nat. Rev. Cancer 6, 583–592.

Prueksaritanont, T., Gorham, L.M., Hochman, J.H., Tran, L.O., Vyas, K.P., 1996. Comparative studies of drug-metabolizing enzymes in dog, monkey, and human small intestines, and in Caco-2 cells. Drug Metab. Dispos. 24, 634–642.

Sambuy, Y., De Angelis, I., Ranaldi, G., Scarino, M.L., Stammati, A., Zucco, F., 2005. The Caco-2 cell line as a model of the intestinal barrier: influence of cell and culture-related factors on Caco-2 cell functional characteristics. Cell Biol. Toxicol. 21, 1–26.

Shin, B.S., Hong, S.H., Hwang, S.W., Kim, H.J., Lee, J.B., Yoon, H.S., Kim do, J., Yoo, S.D., 2009. Determination of zearalenone by liquid chromatography/tandem mass spectrometry and application to a pharmacokinetic study. Biomed. Chromatogr. 23, 1014–1021.

Shin, C.S., Kwak, B., Han, B., Park, K., 2013. Development of an in vitro 3D tumor model to study therapeutic efficiency of an anticancer drug. Mol. Pharmacol. 10, 2167–2175.

Smalley, K.S.M., Lioni, M., Herlyn, M., 2006. Life isn't flat: taking cancer biology to the next dimension. In Vitro Cell. Dev. Biol. 42, 242–247.

Verbeeck, R.K., Richardson, C.J., Blocka, K.L., 1986. Clinical pharmacokinetics of piroxicam. J. Rheumatol. 13, 789–796.

Vesell, E.S., 1974. Relationship between drug distribution and therapeutic effects in man. Annu. Rev. Pharmacol. 14, 249–270.

Youssef, J., Nurse, A.K., Freund, L.B., Morgan, J.R., 2011. Quantification of the forces driving self-assembly of three-dimensional microtissues. Proc. Natl. Acad. Sci. U. S. A. 108, 6993–6998.

Zhu, C., Jiang, L., Chen, T., Hwang, K., 2002. A comparative study of artificial membrane permeability assay for high throughput profiling of drug absorption potential. Eur. J. Med. Chem. 37, 399–407.